Multiscale texture classification using dual-tree complex wavelet transform

Turgay Celik, Tardi Tjahjadi
School of Engineering, University of Warwick,
Gibbet Hill Road, Coventry, CV4 7AL, United Kingdom,
Email: tt@eng.warwick.ac.uk.

Abstract
This paper presents a multiscale texture classifier that exploits the Gabor-like properties of the dual-tree complex wavelet transform, shift invariance and 6 directional subbands at each scale, and uses a feature vector comprising of a variance and an entropy at different scales of each of the directional subbands. Experimental results demonstrate its robustness against noise and a higher classification accuracy than a discrete wavelet transform based classifier.

Keywords:
texture classification, dual-tree complex wavelet transform, multi-resolution analysis

1. Introduction

Numerous methods have been proposed for texture feature extraction and classification (Tuceryan & Jain, 1993). A comparative study (Randen & Husoy, 1999) suggests that for texture classification it is preferable to extract texture features by learning discriminative texture features from texture samples. Most approaches to texture analysis use a hybrid of different methodologies, making it difficult to categorize them. By considering the main methodology used in texture analysis, we can loosely classify them into three main categories (Kim & Kang, 2007).

Statistical approach to texture analysis is motivated from the findings that the human visual system recognizes textured objects based on the statistical distribution of their image grey levels via first-order, second-order, or higher-order statistics (Julesz et al., 1973), (Julesz, 1962). The most commonly used method is the grey-level co-occurrence matrix (Haralick et al., 1973), which estimates texture properties related to the second-order statistics. It is worth pointing out that although statistical textural features are usually used to classify texture regions, most of them are extracted explicitly or implicitly based on a statistical representation of texture.

Model-based approach to texture analysis views textures as mathematical image perceptual models. The key problems with this approach is how to choose a suitable model for characterizing the selected textures and how to estimate the parameters of these models based on some criteria. Another concern is that an intensive computation is usually required to determine the model parameters. The derived parameters are used as the features to capture the perceived essential qualities of the texture. Commonly used texture models include the autoregressive model (AR) (Randen & Husoy, 1999),(Cariou & Chehdi, 2008), Markov random field (MRF) (Cohen et al., 1991), and Wold decomposition model (Liu & Picard, 1996). AR model is a linear model derived from the training samples via a least-mean-squares fitting. Using cliques MRF attempts to describe the relationship of texture pixels within a region of interest. Its optimization is based on maximizing the posteriori probability. Wold decomposition model is a perceptual

texture model that decomposes textures into deterministic and non-deterministic fields, that correspond to regular textural component and random textural component, respectively. Usually, these models can capture the local contextual information in a texture image. However, the model parameters are optimized based on an image representative features instead of its discriminative features.

Signal processing approach to texture analysis includes multichannel Gabor filter, wavelet transform, finite impulse response (FIR) filter, etc. Gabor filter is appealing because of its simplicity and support from neurophysiological experiments (Faugeras, 1978). Gabor filters have been used for texture segmentation despite being based on texture reconstruction (Jain & Farrokhnia, 1991), (Arivazhagan et al., 2006). A general filter bank is often too large because it is designed to capture general texture properties. However, textures can be classified by only a small set of filters, which gives rise to the filter selection problem. For example, a neural network system has been used to select a minimum set of Gabor filters for texture discrimination while keeping the performance at an acceptable level compared to the case without filter selection (Jain & Karu, 1996). In these filtering methods, texture images are usually decomposed into several feature images through projection by using a set of selected filters. These filters are often based on representation such that textures are reconstructed with the minimum information loss. On the other hand, our proposed approach extracts features that maximizes the separation or discrimination among different textures. The wavelet based methods are similar to Gabor based methods with the Gabor filters replaced by Discrete Wavelet Transform (DWT) (Wang et al., 1998), (Laine & Fan, 1993), (Arivazhagan & Ganesa, 2003), (Arivazhagan & Ganesa, 2003, 1), (Muneeswarana et al., 2005), (Kim & Kang, 2007), (Kokare et al., 2007), (Hiremath & Shivashankar, 2008). Since the DWT is shift variance, a shift in the signal degrades the performance of DWT based classifiers.

For the purpose of pattern discrimination, linear Fisher discriminant (Duda et al., 2001) can incorporate feature extraction, dimensionality reduction and discrimination. However its linear optimal solution heavily depends on the assumption that the input patterns have equal covariance matrix. This assumption is usually not true for real data. To overcome this limitation, a kernel version of the Fisher discriminant is recently developed for nonlinear discriminative feature extraction. The optimal solution of the kernel Fisher discriminant corresponds to the optimal Bayesian classifier which accounts for the minimization of the classification (Bayesian) error rate (Schölkopf & Smola, 2002), (Mika et al., 1999). But these methods are computationally expensive.

Since the dual-tree complex wavelet transform (DT-CWT) (Kingsbury, 2001) is a special case of the Gabor filters with complex coefficients it has the directional advantages of the Gabor filters but requiring less computation. Furthermore, it is better than DWT as it is approximately shift invariance and has good directional selectivity in two dimensions. Thus, we propose a computationally efficient multiscale texture classifier using DT-CWT which exploits these advantages. The proposed multiscale texture classifier utilises the benefits of the multiresolution structure of DT-CWT for multiscale feature extraction.

The paper is organized as follows. Section 2 presents DT-CWT. Section 3 presents the proposed multiscale texture classifier, and the learning and classification of texture features for different classes. The experimental results and discussions are presented in Section 4. Finally, Section 5 concludes the paper.

2. Dual-tree complex wavelet transform

Standard DWT's suffer from shift dependence, i.e., the decomposition of image energy between levels of a multiscale decomposition can vary significantly if the original image is shifted prior to decomposition. In order to address the problem of shift variance, complex wavelets have been proposed. A complex wavelet is a set of two real wavelets with a 90° phase difference.

DT-CWT is obtained by filtering an image separably: 2 trees are used for the rows of the image and 2 trees for the columns in a quad-tree structure with 4:1 redundancy. The 4 quad-tree components of each DT-CWT coefficient are combined by simple arithmetic sum and difference operations to yield a pair of complex coefficients (Kingsbury, 2001). This produces 6 directionally selective subbands for each scale

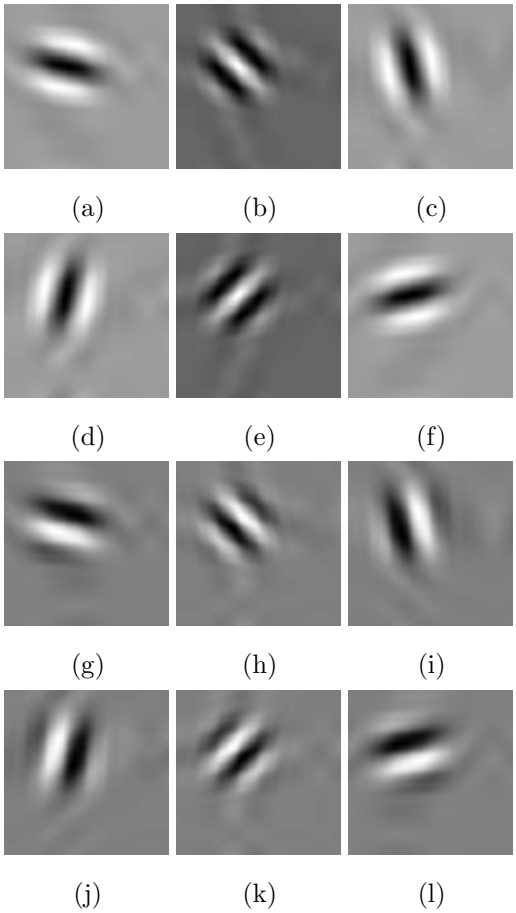

Fig. 1. The real and imaginary parts of the impulse response of the DT-CWT filters for the 6 directional subbands: (a) real, $-15°$; (b) real, $-45°$; (c) real, $-75°$; (d) real, $75°$; (e) real, $45°$; (f) real, $15°$; (g) imaginary, $-15°$; (h) imaginary, $-45°$; (i) imaginary, $-75°$; (j) imaginary, $75°$; (k) imaginary, $45°$; and (l) imaginary, $15°$.

of the 2-dimensional DT-CWT at approximately $\pm 15°, \pm 45°$ and $\pm 75°$ (Kingsbury, 2001). The impulse responses of the filters for the 6 directional subbands are shown in Fig. 1.

Since DT-CWT produces complex coefficients $(R_{i,s}, C_{i,s})$ for each directional subband at each scale, we use the magnitude of the coefficients, i.e.,

$$M_{i,s} = \sqrt{R_{i,s}^2 + C_{i,s}^2} \tag{1}$$

where s refers to scale, $i \in \{\pm 15°, \pm 45°, \pm 75°\}$ is a set of 6 subbands and $M_{i,s}$ is magnitude of the coefficients of subband i at scale s. Fig. 2 shows a sample texture image from the MIT VisTex database (MIT Vison and Modeling Group, 1998) and its $M_{i,1}$,$M_{i,2}$ and $M_{i,3}$. For visualization purpose the magnitude of all subbands have been normalized to $[0, 1]$.

3. The proposed texture classifier

We propose a texture classifier which comprises a texture training stage and a texture classification stage. In the texture training stage, S level DT-CWT is applied to the training texture samples from different texture classes. The subbands of S level DT-CWT are used to form a discriminative feature vector for the multiscale texture classifier. The mean feature vector of the extracted feature vectors for each texture class is calculated and stored in a database for texture classification. In the texture classification stage, for the query texture sample S level DT-CWT is applied to extract discriminative query feature vector. The extracted query feature vector is compared with the mean feature vectors in the feature

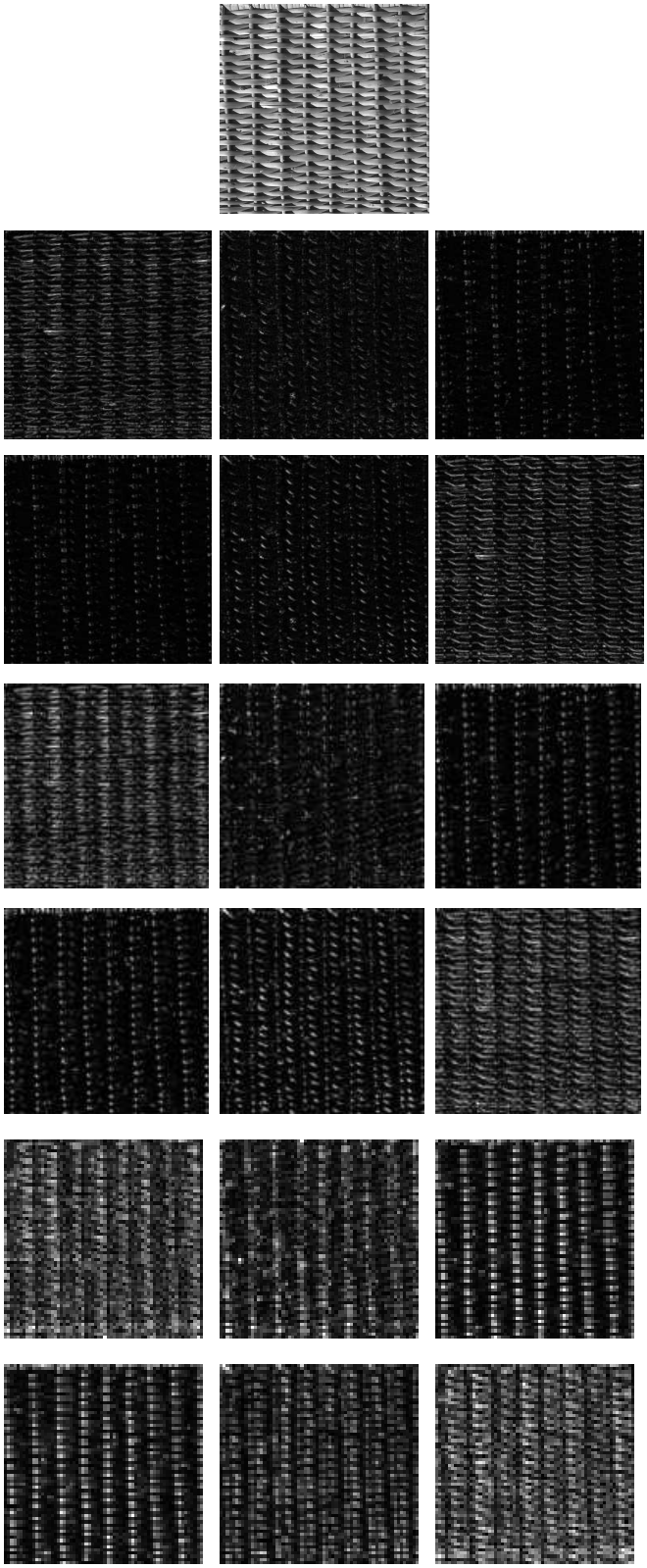

Fig. 2. Magnitude of DT-CWT coefficients in 6 subbands for a texture sample (Fabric.0013) from the MIT VisTex database. The first image is the original image, the next 6 images are $M_{i,1}$, the following 6 images are $M_{i,2}$, and the final 6 images are $M_{i,3}$. For each group of 6 images, the subbands are arranged from left to right in the following directions: $-15°, -45°, -75°, 75°, 45°, 15°$.

database to find the target texture class. The comparison between two feature vectors is performed using a modified Euclidean distance.

3.1. *Feature extraction*

Denote $M_{i,s}(x, y)$ as the magnitude of complex coefficient in directional subband i and scale s, and (x, y) is the spatial location for the corresponding subband with $1 \leq x \leq I$, $1 \leq y \leq J$. We define a variance $v_{i,s}$ and an entropy $e_{i,s}$ (Laine & Fan, 1993) as the features for $M_{i,s}$, i.e.,

$$\mu_{i,s} = \frac{1}{IJ} \sum_{x=1}^{I} \sum_{y=1}^{J} M_{i,s}(x, y) \tag{2}$$

$$v_{i,s} = \frac{1}{IJ} \sum_{x=1}^{I} \sum_{y=1}^{J} (M_{i,s}(x, y) - \mu_{i,s})^2 \tag{3}$$

$$e_{i,s} = -\frac{1}{IJ} \sum_{x=1}^{I} \sum_{y=1}^{J} M_{i,s}(x, y)^2 \log(M_{i,s}(x, y)^2) \tag{4}$$

The variance $v_{i,s}$ is used to measure the spread of the grey-level distribution. It is expected to be large if the grey levels of the image are widely spread out. This feature is used to estimate the contrast of the texture. The entropy $e_{i,s}$ is used to measure the randomness of the grey-level distribution. It is expected to be high if the grey levels are distributed randomly throughout the image. More features can be used for texture classification (Laine & Fan, 1993), however we find that these two features are sufficient to produce a good performance.

The two features are extracted to form a feature vector $\vec{f}_{k,t}$ for test image k from a known texture class t, i.e.,

$$\vec{f}_{k,t} = \frac{[\vec{v}_{\pm[a,b,c],1} \cdots \vec{v}_{\pm[a,b,c],s}\ \vec{e}_{\pm[a,b,c],1} \cdots \vec{e}_{\pm[a,b,c],S}]}{\sqrt{2S}} \tag{5}$$

where $a = 15°$, $b = 45°$, $c = 75°$, S is the number of scales used in DT-CWT, and

$$\vec{v}_{\pm[a,b,c],s} = \frac{[v_{-a,s}\ v_{-b,s}\ v_{-c,s}\ v_{c,s}\ v_{b,s}\ v_{a,s}]}{\sqrt{v_{-a,s}^2 + v_{-b,s}^2 + v_{-c,s}^2 + v_{c,s}^2 + v_{b,s}^2 + v_{a,s}^2}} \tag{6}$$

$$\vec{e}_{\pm[a,b,c],s} = \frac{[e_{-a,s}\ e_{-b,s}\ e_{-c,s}\ e_{c,s}\ e_{b,s}\ e_{a,s}]}{\sqrt{e_{-a,s}^2 + e_{-b,s}^2 + e_{-c,s}^2 + e_{c,s}^2 + e_{b,s}^2 + e_{a,s}^2}} \tag{7}$$

At each scale we extract 12 features, 6 for $\vec{v}_{\pm[a,b,c],s}$ and 6 for $\vec{e}_{\pm[a,b,c],s}$. Thus, $\vec{f}_{k,t}$ is a vector with $12S$ elements.

3.2. *Texture learning and classification using DT-CWT*

In order to perform a supervised texture classification using DT-CWT, the following learning stage for the texture classifier is required:

(i) Decompose a training texture image using S levels of DT-CWT and normalize each subband by its energy;
(ii) For each scale s, use Eq. (5) to generate the feature vector for each directional subband;
(iii) Repeat steps (i) and (ii) for all sample images in the same texture class;
(iv) Generate the mean and variance of the feature l for each texture class t, i.e., $fm_{t,l}$ and $\sigma_{t,l}$, respectively, for the training samples and store them in the database;

(v) Repeat the above steps for each different texture image in the training stage.

After the features have been learned for each texture class, the following classification stage is performed:

(i) Decompose an unknown texture image using S levels of DT-CWT and extract its feature vector using step (i) and (ii) of the learning stage, denoting the feature vector by $\vec{f^u}$;

(ii) Calculate the distance between $\vec{f^u}$ and the mean feature vector $\vec{fm}_t$ of each class t using

$$D_c = \mathrm{d}(\vec{f^t}, \vec{fm}_t) \tag{8}$$

where d( ) is distance or discrimination function and

$$\vec{fm}_t = \frac{1}{L}\sum_{k=1}^{L} \vec{f}_{k,t} \tag{9}$$

where L is the number of texture samples used in training;

(iii) Assign the unknown texture to texture class $\tilde{t}$ if $D_{\tilde{t}} < D_t$ for all $\tilde{t} \neq t$.

The discrimination function is

$$\mathrm{d}(\vec{f^u}, \vec{fm}_t) = \sum_{l=1}^{12S} \frac{(f_l^u - fm_{t,l})^2}{\sigma_{t,l}} \tag{10}$$

where f_l^u is the feature l of the test image, and $\sigma_{t,l}$ is the standard deviation of the feature $fm_{t,l}$. Eq. (10) means that features with small variances are more informative than features with high variances, and thus it enhances features with small variances and degrades those with high variances.

4. Experimental results and discussion

The effectiveness of the proposed texture feature extraction approach to texture classification is evaluated by performing supervised classification of several test images with varying texture complexities from two commonly-used natural texture image databases: MIT VisTex database (MIT Vison and Modeling Group, 1998) and Brodatz album (Brodatz, 1966). Each texture image has a size of 512×512, with 256 grey levels. Each image is globally histogram equalized and normalized to [-1,1] to ensure that the textures are not trivially discriminable simply based on the local mean or local variance. Different portions of the input patterns of each texture class are selected and used for training the texture classifier. We avoid using the texture patterns on a texture border for training because these patterns are not representative of the texture.

Twelve images containing similar textural patterns (thus making classification more difficult) from each of the MIT VIS-Tex database and Brodatz album as respectively shown in Fig. 3 and Fig. 4 are used. A hybrid texture database is formed by including all the twenty-four texture samples from both databases. Each texture image is divided into two non-overlapping parts of size 256×512, one for training and one for testing. Overlapped samples are generated from the training texture images using a sliding window of size $K \times K$ which is moved with shifts of Δ in both the horizontal and vertical directions. The number of test samples varies with the value of Δ. The value of Δ is set to 4 to give a reasonable overlap between two test samples, thus a total of 3072 texture samples are used in training for each class. After training, another 3072 samples are used to evaluate the performance of the texture classifier.

The performance of a texture classifier is measured using a confusion matrix (Kohavi & Provost, 1998) **CM**. **CM** is a $L \times L$ matrix for L different texture classes and $\mathbf{CM}(i, j)$ refers to the classification rate when samples from class i are identified as class j. Two figure of merits are used in conjunction with **CM**: average correct classification rate $accr$ and average false classification rate $afcr$, where

$$accr = \frac{1}{L}\sum_{\forall(i,j), i=j} \mathbf{CM}(i, j) \tag{11}$$

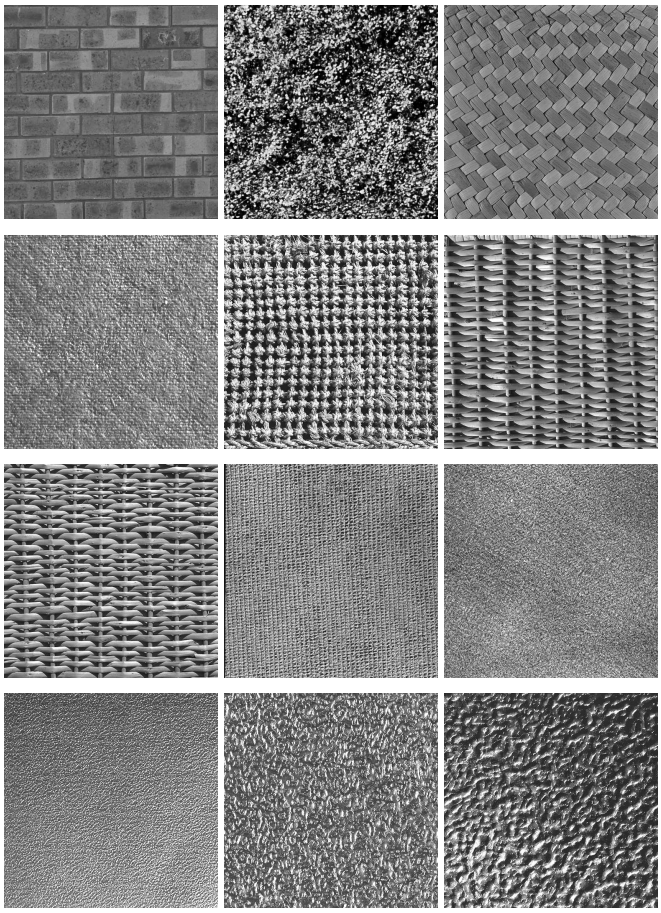

Fig. 3. Texture samples from the MIT VisTex database: Brick.0001 (m_1); Leaves.0003 (m_2); Fabric.0001 (m_3); Fabric.0007 (m_4); Fabric.0009 (m_5); Fabric.0013 (m_6); Fabric.0014 (m_7); Fabric.0017 (m_8); Fabric.0018 (m_9); Metal.0001 (m_{10}); Metal.0002 (m_{11}); and Metal.0005 (m_{12}).

$$afcr = \frac{1}{L \times (L-1)} \sum_{\forall(i,j), i \neq j} \mathbf{CM}(i,j) \tag{12}$$

We performed experiments to evaluate the effects of the number of scales S and Gaussian noise on the proposed multiscale texture classifier using DT-CWT. In order to make comparisons with DWT, the same structure of the proposed multiscale texture classifier is applied to DWT where the features are extracted from the high-pass subbands. DWT produces three subbands at each scale which are directional at 0°, 45° and 90°. The same features as in Eq. (3) and (4) are used for each directional subband. For each scale and for S levels of DTW, 6 (i.e., 3×2) features are extracted, giving a total of $6S$ features.

In general DWT based texture feature descriptors use similar features as defined in Eq. (3) and (4) but with different formulations, e.g., (Arivazhagan & Ganesa, 2003), (Arivazhagan & Ganesa, 2003, 1), (Muneeswarana et al., 2005). Thus, if we show that our proposed feature vector performs better in DT-CWT than in DWT, then it is highly expected that if the features used in DWT based classifiers are employed in our DT-CWT based multiscale classifier then they will also perform better.

4.1. *The effects of the number of scales*

Using the images from the MIT VisTex database (MIT Vison and Modeling Group, 1998), the first experiment determines the effects of the number of scales S used for the feature vector $\vec{f}_{k,t}$. The top half of Table 1 shows the confusion matrices for different values of S. The results for the MIT VisTex database in Table 2 shows that the $accr$ for $S = 1$ is 94.8% while the $afcr$ is as high as 0.5%. When $S = 2$ the $accr$ increases to 99.3% while the $afcr$ decreases to 0.1%. A further improvement is achieved with $S = 3$

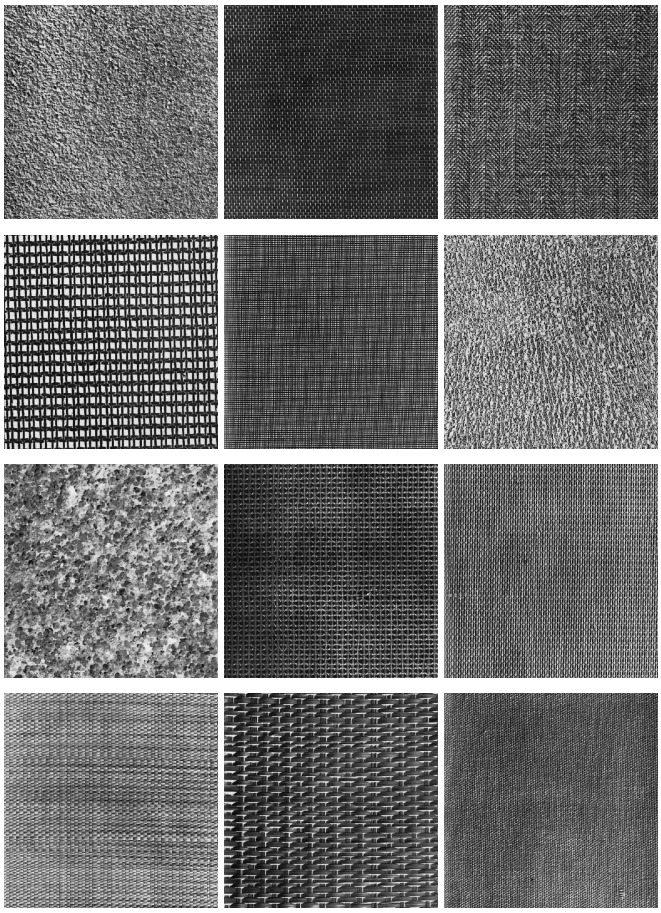

Fig. 4. Texture samples from the Brodatz album: D4 (b_1); D6 (b_2); D17 (b_3); D20 (b_4); D21 (b_5); D24 (b_6); D28 (b_7); D52 (b_8); D53 (b_9); D55 (b_{10}); D65 (b_{11}); and D77 (b_{12}).

where the $accr$ and $afcr$ are respectively 100% and 0%. Fig. 5 (a) and (b) respectively show with solid lines the $accr$ and $afcr$ with respect to the number of scales used. It is clear that $S = 3$ gives the best correct classification with low false classification.

The same test is applied to the twelve images from the Brodatz album (Brodatz, 1966) as shown in Fig. 4. The lower half of Table 1 shows the confusion matrices for different values of S. The results for the Brodatz album in Table 2 shows that the $accr$ for $S = 1, 2, 3$ are respectively 96.2%, 99.9% and 100%. The $afcr$ for $S = 1, 2, 3$ are respectively 0.3%, 0.01% and 0%. The $accr$ and $afcr$ with respect to the number of scales used are shown with solid lines in Fig. 5 (c) and (d), respectively. It is clear that $S = 3$ gives the best correct classification with low false classification.

The confusion matrices for the DWT are shown in Table 3 for the two test sets of images. The results when compared with those of the DT-CWT based classifier (as shown in Table 2) show that the discrimination power of DT-CWT is higher than DWT. The overall classification of DT-CWT and DWT with respect to the number of scales used are shown in Fig. 5. It is clear from Fig. 5 and Table 2 that the DT-CWT based texture classifier outperforms the DWT based texture classifier by having high $accr$ and low $afcr$ for both sets of texture images. The exception occurs when $S = 3$ for the Brodatz album where the performance of both algorithms are the same.

Increasing the number of scales beyond $S = 3$ may improve the performance of the proposed classifier. However, the decimated wavelet transform halves the size of a subband at each new coarser scale. This effect results in not having sufficient discriminating data beyond some scales. For instance, if the size of the texture image is 64×64, when $S = 4$ the coarser scale has 4 coefficients to extract features. This number may not be sufficient for discriminative feature extraction. This drawback may be overcome by using more

Table 1
Confusion matrices for DT-CWT for different number of scales used S on texture samples of class m_n from the MIT VisTex database and of class b_n from the Brodatz album with $\Delta = 4$, i.e., 3072 training and test samples.

MIT VisTex database

S=1	m_1	m_2	m_3	m_4	m_5	m_6	m_7	m_8	m_9	m_{10}	m_{11}	m_{12}
m_1	100	0	0	0	0	0	0	0	0	0	0	0
m_2	1.6	97.3	0	0	0	0	0	1.2	0	0	0	0
m_3	0	0	99.6	0	0	0	0	0	0	0	0	0.4
m_4	4.4	0	0	95.6	0	0	0	0	0	0	0	0
m_5	0	0	0	0	82.6	0	0	0	17.4	0	0	0
m_6	0	0	0	0	0	100	0	0	0	0	0	0
m_7	0	0	0	0	0	0	100	0	0	0	0	0
m_8	0	0	0	0	0	0	0	100	0	0	0	0
m_9	0	0	0	0	0	0	0	0	62.8	0	37.2	0
m_{10}	0	0	0	0	0	0	0	0	0	100	0	0
m_{11}	0	0	0	0	0	0	0	0	0	0	100	0
m_{12}	0	0	0	0	0	0	0	0	0	0	0	100

S=2	m_1	m_2	m_3	m_4	m_5	m_6	m_7	m_8	m_9	m_{10}	m_{11}	m_{12}
m_1	100	0	0	0	0	0	0	0	0	0	0	0
m_2	0	100	0	0	0	0	0	0	0	0	0	0
m_3	0	0	100	0	0	0	0	0	0	0	0	0
m_4	0	0	0	100	0	0	0	0	0	0	0	0
m_5	0	0	0	0	100	0	0	0	0	0	0	0
m_6	0	0	0	0	0	100	0	0	0	0	0	0
m_7	0	0	0	0	0	0	100	0	0	0	0	0
m_8	0	0	0	0	0	0	0	100	0	0	0	0
m_9	0	0	0	0	0	0	0	0	100	0	0	0
m_{10}	0	0	0	0	0	0	0	0	0	91.5	0	8.5
m_{11}	0	0	0	0	0	0	0	0	0	0	100	0
m_{12}	0	0	0	0	0	0	0	0	0	0	0	100

S=3	m_1	m_2	m_3	m_4	m_5	m_6	m_7	m_8	m_9	m_{10}	m_{11}	m_{12}
m_1	100	0	0	0	0	0	0	0	0	0	0	0
m_2	0	100	0	0	0	0	0	0	0	0	0	0
m_3	0	0	100	0	0	0	0	0	0	0	0	0
m_4	0	0	0	100	0	0	0	0	0	0	0	0
m_5	0	0	0	0	100	0	0	0	0	0	0	0
m_6	0	0	0	0	0	100	0	0	0	0	0	0
m_7	0	0	0	0	0	0	100	0	0	0	0	0
m_8	0	0	0	0	0	0	0	100	0	0	0	0
m_9	0	0	0	0	0	0	0	0	100	0	0	0
m_{10}	0	0	0	0	0	0	0	0	0	100	0	0
m_{11}	0	0	0	0	0	0	0	0	0	0	100	0
m_{12}	0	0	0	0	0	0	0	0	0	0	0	100

Brodatz album

S=1	b_1	b_2	b_3	b_4	b_5	b_6	b_7	b_8	b_9	b_{10}	b_{11}	b_{12}
b_1	100	0	0	0	0	0	0	0	0	0	0	0
b_2	0	59.1	29.7	0	11.2	0	0	0	0	0	0	0
b_3	0	0	96.0	0	0	0	0	4.0	0	0	0	0
b_4	0	0	0	100	0	0	0	0	0	0	0	0
b_5	0	0	0	0	100	0	0	0	0	0	0	0
b_6	0	0	0	0	0	100	0	0	0	0	0	0
b_7	0	0	0	0	0	0	100	0	0	0	0	0
b_8	0	0	0	0	0	0	0	100	0	0	0	0
b_9	0	0	0	0	0	0	0	0	100	0	0	0
b_{10}	0	0	0	0	0	0	0	0	0	100	0	0
b_{11}	0	0	0	0	0	0	0	0	0	0.3	99.7	0
b_{12}	0	0	0	0	0	0	0	0	0	0	0	100

S=2	b_1	b_2	b_3	b_4	b_5	b_6	b_7	b_8	b_9	b_{10}	b_{11}	b_{12}
b_1	100	0	0	0	0	0	0	0	0	0	0	0
b_2	0	100	0	0	0	0	0	0	0	0	0	0
b_3	0	0	99.2	0	0	0	0.4	0.4	0	0	0	0
b_4	0	0	0	100	0	0	0	0	0	0	0	0
b_5	0	0	0	0	100	0	0	0	0	0	0	0
b_6	0	0	0	0	0	100	0	0	0	0	0	0
b_7	0	0	0	0	0	0	100	0	0	0	0	0
b_8	0	0	0	0	0	0	0	100	0	0	0	0
b_9	0	0	0	0	0	0	0	0	100	0	0	0
b_{10}	0	0	0	0	0	0	0	0	0	100	0	0
b_{11}	0	0	0	0	0	0	0	0	0	0	100	0
b_{12}	0	0	0	0	0	0	0	0	0	0	0	100

S=3	b_1	b_2	b_3	b_4	b_5	b_6	b_7	b_8	b_9	b_{10}	b_{11}	b_{12}
b_1	100	0	0	0	0	0	0	0	0	0	0	0
b_2	0	100	0	0	0	0	0	0	0	0	0	0
b_3	0	0	100	0	0	0	0	0	0	0	0	0
b_4	0	0	0	100	0	0	0	0	0	0	0	0
b_5	0	0	0	0	100	0	0	0	0	0	0	0
b_6	0	0	0	0	0	100	0	0	0	0	0	0
b_7	0	0	0	0	0	0	100	0	0	0	0	0
b_8	0	0	0	0	0	0	0	100	0	0	0	0
b_9	0	0	0	0	0	0	0	0	100	0	0	0
b_{10}	0	0	0	0	0	0	0	0	0	100	0	0
b_{11}	0	0	0	0	0	0	0	0	0	0	100	0
b_{12}	0	0	0	0	0	0	0	0	0	0	0	100

Table 2
Classification rates of the proposed classifier in (%) using DT-CWT and DWT for the MIT VisTex database, the Brodatz album, and the Hybrid database.

	MIT VisTex database				Brodatz album				Hybrid database			
	DT-CWT		DWT		DT-CWT		DWT		DT-CWT		DWT	
S	$accr$	$afcr$	$accr$	$afcr$	$accr$	$afcr$	$accr$	$afcr$	$accr$	$afcr$	$accr$	$afcr$
1	94.8	0.5	76.5	2.1	96.2	0.3	77.8	2.0	90.4	0.4	76.4	1.0
2	99.3	0.1	92.3	0.7	99.9	0.01	92.4	0.7	99.1	0.03	90.7	0.4
3	100	0	98.1	0.2	100	0.0	100	0.0	100	0.0	99.0	0.04
4	99.8	0.01	94.1	0.5	100	0.0	98.3	0.2	99.9	0.004	93.8	0.3

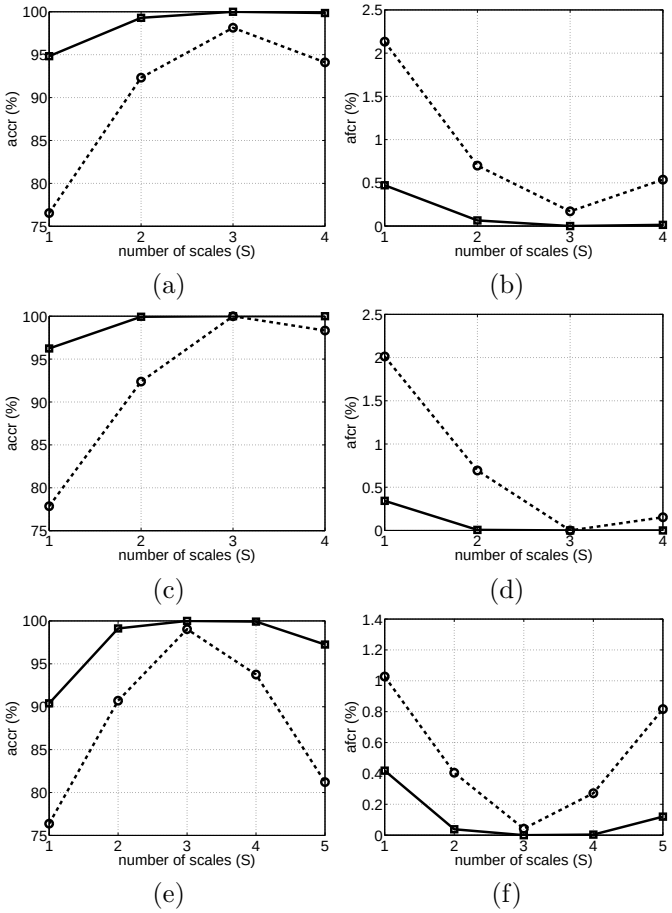

Fig. 5. Comparison between the classification rates of DT-CWT (solid lines) and DWT (dashed lines) for different databases: (a) average correct classification for the MIT VisTex database; (b) average false classification for the MIT VisTex database; (c) average correct classification for the Brodatz album; (d) average false classification for the Brodatz album; (e) average correct classification for the Hybrid database; and (f) average false classification for the Hybrid database.

features or use non-decimated wavelet transform. The effect of this phenomenon and the effectiveness of the proposed classifier for inter-database discrimination are evaluated on the Hybrid texture database. The results are shown in Fig. 5 (e) for $accr$, Fig. 5 (f) for $afcr$ and in Table 2. It is clear from Fig. 5 (e) and (f) that the proposed classifier in DT-CWT domain outperforms the proposed classifier in DWT domain. It is noticeable that, the proposed classifier in DT-CWT domain does not degrades its performance as much as in DWT domain while S increases. The proposed classifier provides 100% performance when $S = 3$ but the performance degrades for $S > 4$.

4.2. *The effects of noise*

The effects of noise on the proposed texture classifier in the DT-CWT and DWT domains are evaluated by adding Gaussian noise with zero mean and different variances to the test images. The classifier for each texture class is trained on the samples without noise. The trained texture classifiers are then tested

Table 3
Confusion matrices for DWT for different number of scales used S on texture samples of class m_n from the MIT VisTex database and of class b_n from the Brodatz album with $\Delta = 4$, i.e., 3072 training and test samples.

MIT VisTex database

S=1	m_1	m_2	m_3	m_4	m_5	m_6	m_7	m_8	m_9	m_{10}	m_{11}	m_{12}
m_1	79.9	0	0	0	0.4	0	0	19.7	0	0	0	0
m_2	0	100	0	0	0	0	0	0	0	0	0	0
m_3	0	0	100	0	0	0	0	0	0	0	0	0
m_4	0	0	0	100	0	0	0	0	0	0	0	0
m_5	0	0	0	0	17.2	0	0	0	53.0	29.8	0	0
m_6	0	0	0	0	0	76.8	23.0	0.1	0	0	0	0
m_7	0	0	0	0	0	0	100	0	0	0	0	0
m_8	88.0	0	0	0	0	0	0	12.0	0	0	0	0
m_9	0	0	0	0	0	0	0	0	100	0	0	0
m_{10}	0	0	0	0	0	0	0	0	57.8	42.2	0	0
m_{11}	0	0	0	0	0	0	0	0	0	0	100	0
m_{12}	0	0	0	0	0	0	0	0	9.0	0	0.7	90.4

S=2	m_1	m_2	m_3	m_4	m_5	m_6	m_7	m_8	m_9	m_{10}	m_{11}	m_{12}
m_1	85.0	0	0	0	0	0	0	15.0	0	0	0	0
m_2	0	100	0	0	0	0	0	0	0	0	0	0
m_3	0	0	99.2	0	0	0	0	0	0	0.8	0	0
m_4	0	0	0	100	0	0	0	0	0	0	0	0
m_5	0	0	0	0	100	0	0	0	0	0	0	0
m_6	0	0	0	0	0	91.1	8.9	0	0	0	0	0
m_7	0	0	0	0	0	0	100	0	0	0	0	0
m_8	0.4	0	0	0	0	0	0	99.6	0	0	0	0
m_9	0	0	0	0	0	0	0	0	100	0	0	0
m_{10}	0	0	0	0	0	0	0	0	67.1	32.9	0	0
m_{11}	0	0	0	0	0	0	0	0	0	0	100	0
m_{12}	0	0	0	0	0	0	0	0	0	0	0	100

S=3	m_1	m_2	m_3	m_4	m_5	m_6	m_7	m_8	m_9	m_{10}	m_{11}	m_{12}
m_1	100	0	0	0	0	0	0	0	0	0	0	0
m_2	0	100	0	0	0	0	0	0	0	0	0	0
m_3	0	0	100	0	0	0	0	0	0	0	0	0
m_4	0	0	0	100	0	0	0	0	0	0	0	0
m_5	0	0	0	0	100	0	0	0	0	0	0	0
m_6	0	0	0	0	0	100	0	0	0	0	0	0
m_7	0	0	0	0	0	8.6	91.4	0	0	0	0	0
m_8	1.6	0	0	0	0	0	0	98.4	0	0	0	0
m_9	0	0	0	0	0	0	0	0	100	0	0	0
m_{10}	0	0	0	0	0	0	0	0	0	100	0	0
m_{11}	0	0	0	0	0	0	0	0	0	0	100	0
m_{12}	0	0	0	0	12.2	0	0	0	0	0	0	87.8

Brodatz album

S=1	b_1	b_2	b_3	b_4	b_5	b_6	b_7	b_8	b_9	b_{10}	b_{11}	b_{12}
b_1	39.3	0	0	0	0	0	4.3	20.7	0	0	0	35.7
b_2	0	28.9	71.0	0	0.1	0	0	0	0	0	0	0
b_3	0	0	100	0	0	0	0	0	0	0	0	0
b_4	0	0	0	100	0	0	0	0	0	0	0	0
b_5	0	0	0	0	100	0	0	0	0	0	0	0
b_6	0	0	0	0	0	100	0	0	0	0	0	0
b_7	24.3	0	0	0	0	0	34.4	0	0	0	0	41.3
b_8	13.5	0	0	0	0	0	0.1	86.3	0	0	0	0
b_9	0	0	0	0	0	0	0	0	100	0	0	0
b_{10}	0	0	0	0	0	0	0	0	0	100	0	0
b_{11}	0	0	0	0	0	0	0	0	0	0	100	0
b_{12}	16.9	0	0	0	0	0	34.1	3.6	0	0	0	45.3

S=2	b_1	b_2	b_3	b_4	b_5	b_6	b_7	b_8	b_9	b_{10}	b_{11}	b_{12}
b_1	99.9	0	0	0	0	0	0.1	0	0	0	0	0
b_2	0	100	0	0	0	0	0	0	0	0	0	0
b_3	0	0	100	0	0	0	0	0	0	0	0	0
b_4	0	0	0	100	0	0	0	0	0	0	0	0
b_5	0	0	0	0	100	0	0	0	0	0	0	0
b_6	0	0	0	0	0	100	0	0	0	0	0	0
b_7	0	0	0	0	0	0	99.3	0	0	0	0	0.7
b_8	0	0	0.1	0	0	0	83.5	16.1	0	0	0	0.3
b_9	0	0	0	0	0	0	0	0	100	0	0	0
b_{10}	0	0	0	0	0.5	0	0	0	0	93.6	5.9	0
b_{11}	0	0	0	0	0	0	0	0	0	0	100	0
b_{12}	0	0	0.4	0	0	0	0	0	0	0	0	99.6

S=3	b_1	b_2	b_3	b_4	b_5	b_6	b_7	b_8	b_9	b_{10}	b_{11}	b_{12}
b_1	100	0	0	0	0	0	0	0	0	0	0	0
b_2	0	100	0	0	0	0	0	0	0	0	0	0
b_3	0	0	100	0	0	0	0	0	0	0	0	0
b_4	0	0	0	100	0	0	0	0	0	0	0	0
b_5	0	0	0	0	100	0	0	0	0	0	0	0
b_6	0	0	0	0	0	100	0	0	0	0	0	0
b_7	0	0	0	0	0	0	100	0	0	0	0	0
b_8	0	0	0	0	0	0	0	100	0	0	0	0
b_9	0	0	0	0	0	0	0	0	100	0	0	0
b_{10}	0	0	0	0	0	0	0	0	0	100	0	0
b_{11}	0	0	0	0	0	0	0	0	0	0	100	0
b_{12}	0	0	0	0	0	0	0	0	0	0	0	100

Table 4
The average classification rates in (%) of DT-CWT and DWT in the present of various noise levels for the Brodatz album when $S = 3$.

SNR (dB)	DT-CWT		DWT	
	accr	***afcr***	***accr***	***afcr***
10	27.1	6.6	23.2	7.0
15	39.4	5.5	33.4	6.0
20	73.6	2.4	53.5	4.2
25	90.6	0.9	79.8	1.8
30	96.9	0.3	92.5	0.7
35	99.6	0.04	98.1	0.2
40	99.97	0.002	98.61	0.13
45	100	0	100	0
50	100	0	100	0

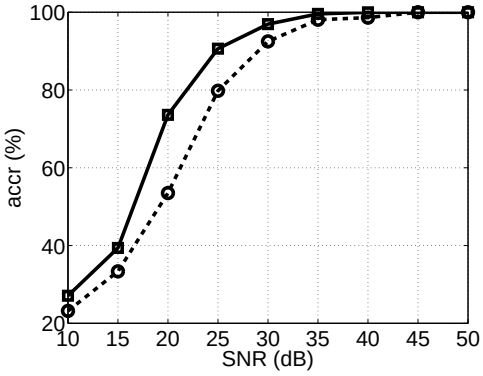

(a)

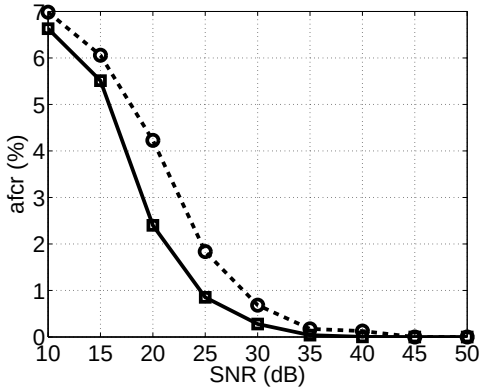

(b)

Fig. 6. Comparison between the classification rates of DT-CWT (solid lines) and DWT (dashed lines) in the present of various noise levels for the Brodatz album when $S = 3$: (a) average correct classification rate; and (b) average false classification rate.

against the noisy test images. The afore mentioned procedure to create the training and test databases is used with the noisy test images. At each noise level, the experiment is repeated 5 times and the average of the 5 results is taken as the performance of the classifier.

The correct and false classification rates versus different noise levels (SNR) are shown in Table 4 and Fig. 6 for the Brodatz album. The Brodatz album is selected for testing because both the DT-CWT and DWT based multiscale texture classifiers achieve the same performance when $S = 3$. We chose $S = 3$ for this test since it gives the highest *accr* and the lowest $afcr$ (see Table 2 and Fig. 5 (c) and (d)). It is clear from Fig. 6 that both classifiers perform well up to a noise level of 25 dB where the *accr* is about 91% and the $afcr$ is 0.9%. At this noise level, the DWT based multiscale classifier shows a weaker performance where the *accr* is about 80% and the $afcr$ is 1.8%. Both classifiers show robust performance with noise level above 35 dB where the performance of the DT-CWT and DWT based multiscale classifiers are about 100% and about 98%, respectively. Thus from Fig. 6 and Table 4, we can conclude that the DT-CWT based multiscale classifier achieves a better performance than the DWT based multiscale classifier.

5. Conclusion

In this paper we propose a novel algorithm for texture classification using DT-CWT. The proposed texture classifier achieves an average correct classification rate of 100% and an average false classification rate of 0% for $S = 3$ on two sets of texture samples of varying complexities and a hybrid test set. This performance shows that the proposed variance and entropy as features of the magnitude of the DT-CWT complex coefficients in 6 directional subbands for 3 scales are good candidates for texture classification. The proposed classifier utilises the benefits of multiscale structure of DT-CWT. The performance of the proposed classifier has also been shown to be robust against noise. The multiscale structure of the proposed classifier not only makes it robust against noise but also improves its ability to make better discrimination between textures.

We also compared the performance of the proposed DT-CWT classifier with the DWT based classifier, and show that the former outperforms the latter by achieving high correct classification rate and low false classification rate. Furthermore, the proposed classifier is more robust against noise in DT-CWT domain than DWT domain.

In this study, we have only used two simple but effective features for texture classification. The spatial information of textures can be used to further improve the performance of the classifier, which will be our future work. We also expect that including the phase information of DT-CWT will improve the classification. Furthermore, we have not employed any feature selection prior to classification. We expect that the feature selection procedure by employing PCA or ICA (Duda et al., 2001) will improve the performance of the proposed texture classifier on larger databases. This will also be our future work.

Acknowledgments

The authors would like to thank Warwick University Vice Chancellor Scholarship for providing the funds for this research.

References

Arivazhagan, S., Ganesan, L., 2003. Texture classification using wavelet transform. Pattern Recognit. Letts. 24, 1513–1521.

Arivazhagan, S., Ganesan, L., 2003 (1). Texture segmentation using wavelet transform. Pattern Recognit. Letts. 24, 3197-3203.

Arivazhagan, S., Ganesan, L., Padam Priyal, S., 2006. Texture classification using Gabor wavelets based rotation invariant features. Pattern Recognit. Letts. 27, 1976–1982.

Brodatz, P. 1966. Textures: A Photographic Album for Artists and Designers. Dover, New York, USA. http://www.ux.his.no/∼tranden/brodatz.html.

Cariou, C., Chehdi, J., 2008. Unsupervised texture segmentation/classification using 2-D autoregressive modeling and the stochastic expectation-maximization algorithm. Pattern Recognit. Letts. 29, 905–917.

Cohen, F., Fan, Z., Patel, M., 1991. Classifcation of rotated and scaled textured images using gaussian markov random field models. IEEE Trans. Pattern Anal. Mach. Intell. 13 (2), 192–202.

Duda, R.O., Hart, P.E., Stork, D.G., 2001. Pattern Classification (2nd ed.). John Wiley and Sons.

Faugeras, O., 1978. Texture analysis and classification using a human visual model. In: Proc. IEEE Int. Conf. Pattern Recognit., 549–552, 1978.

Haralick, R., Shangmugam, K., Dinstein, L., 1973. Textural features for image classification. IEEE Trans. Sys. Man Cybern. 3, 610–621.

Hiremath, P.S., Shivashankar, S., 2008. Wavelet based co-occurrence histogram features for texture classification with an application to script identification in a document image. Pattern Recognit. Letts. 29, 1182–1189.

Jain, A., Farrokhnia, F., 1991. Unsupervised texture segmentation using Gabor filters. Pattern Recognit. 24 (12), 1167–1186.

Jain, A. Karu, K., 1996. Learning texture discrimination masks. IEEE Trans. Pattern Anal. Mach. Intell. 18 (2), 195–205.

Julesz, B., 1962. Visual pattern discrimination. IRE Trans. on Information Theory 8 (2), 84-92.

Julesz, B., Gilbert, E.N., Shepp, L.A., Frisch, H.L., 1973. Inability of humans to discriminate between visual textures that agree in second-order statistics – revisited. Perception 1 (2) , 391–405.

Kim, S.C., Kang, T.J., 2007. Texture classification and segmentation usingwavelet packet frame and Gaussian mixture model. Pattern Recognit. 40, 1207–1221.

Kingsbury, N.G., 2001. Complex wavelets for shift invariant analysis and filltering of signals. Journal of Applied and Computational Harmonic Analysis 3, 234–253.

Kohavi, R., Provost, F., 1998. Glossary of Terms. Machine Learning 30 (2/3), 271–274.

Kokare, M., Biswas, P.K., Chatterji, B.N., 2007. Texture image retrieval using rotated wavelet filters. Pattern Recognit. Letts. 28, 1240–1249.

Laine, A., Fan, J., 1993. Texture classification by wavelet packet signatures. IEEE Trans. Pattern Anal. Mach. Intell. 15 (11), 1186–1191.

Liu, F., Picard, R., 1996. Periodicity, directionality, and randomness: Wold features for image modeling and retrieval. IEEE Trans. Pattern Anal. Mach. Intell. 18 (7), 722–733.

Mika, S., Rätsch, G., Weston, J., Schölkopf, B., Müller, K.R., 1999. Fisher discriminant analysis with kernels. In: Proceedings of the 1999 IEEE Signal Processing Society Workshop, 41–48.

MIT Vision and Modelling Group, 1998. http://www.media.mit.edu/vismod/.

Muneeswarana, K., Ganesanb, L., Arumugamc, S., Soundara, K.R., 2005. Texture classification with combined rotation and scale invariant wavelet features. Pattern Recognit. 38, 1495–1506.

Randen, T., Husoy, J., 1999. Filtering for texture classification: A comparative study. IEEE Trans. Pattern Anal. Mach. Intell. 21 (4), 291–310.

Schölkopf, B., Smola, A.J., 2002. Learning with Kernels: Support Vector Machines, Regularization, Optimization and Beyond. Cambridge, MA: MIT Press.

Tuceryan, M., Jain, A., 1993. Texture analysis. In: Handbook of Pattern Recognition and Computer Vision, Chen, C., Pau, L., Wang, P. (Eds.). Singapore: World Scientific, 235–276.

Wang, J.W., Chen, C.H., Chien, Chien, W.M., Tsai, C.M., 1998. Texture classification using non-separable two-dimensional wavelets. Pattern Recognit. Letts. 19, 1225–1234.